Precise Network Polymerized Ionic Liquids for Low-Voltage, Dopant-Free Soft Actuators

*Chengtian Shen, Qiujie Zhao, and Christopher M. Evans**

Next-generation material applications require electroactive materials for actuation which are light weight, operate at low voltages (<5 V), exhibit cyclability, and are compatible with a range of environments. Here, a class of network polymerized ionic liquid (n-PIL) actuators is reported, synthesized via a facile step growth polymerization, which not only have comparable actuation strains (≈0.9%) to other state-of-the-art ionic polymer systems at ±3 V, but also exhibit 85% performance preservation after 1000 testing cycles and operate with no additives such as solvent or free ionic liquid. Molecular engineering of the n-PILs by controlling crosslinking density and linker polarity leads to an order-of-magnitude increase in tip displacement which provides insights on future materials development.

Soft actuators are currently receiving intense interest in a diverse range of fields including soft robotics, artificial muscles, and tactile communication.[1–16] The primary requirements are that the actuator is lightweight, flexible, fast, and generates either a significant force or displacement depending on the application. Secondary requirements often include low power consumption (for untethered operation), high cycling capability, and low cost. Over the past 2 decades, dielectric elastomer actuators,[6,17–20] typically with poly(dimethylsiloxane) (PDMS) as the dielectric layer, have received attention for their fast response and substantial strains, in particular under biaxial expansion. Generally, they require kV potentials although the corresponding current is low.[17,18] At such high fields, electrostriction is the dominant mechanism of actuation where opposing electrodes are attracted to each other and the elastomer deforms in response to this pressure. This mechanism appears to be well suited to biaxial strains which can exceed 100% in the plane of the film.[17] However, demonstrations of bending with dielectric elastomers using electric fields are rare.

Actuation using nonelectrical stimuli, such as solvent swelling/deswelling,[21–25] temperature,[26] and pH[3,27] are also investigated. However, low voltage stimuli would be ideal because the application of potential is fast, easy to miniaturize, and suitable for interfacing with the skin. Thus, this motivates a sustained interest in the pursuit of low-voltage actuators. Ionic polymer metal composites (IPMCs)[28–33] are a widely studied system where a polymer such as Nafion, which contains hydrated acid groups and water channels within a fluorocarbon matrix, is sandwiched between Pt electrodes via electroless plating. Ionic actuators operate at low voltage (1–5 V) but with mA currents (rather than μAs in dielectric elastomers) as ions migrate to the electrodes. Hydrated systems exhibit high conductivity and fast response but suffer from water splitting and dehydration issues at higher potentials leading to poor cyclability. They also exhibit "back relaxation," a phenomenon where an actuator beam will first deform to some extent and then slowly migrate back to the origin even with a steady applied voltage.[34] Recent strategies in ionic actuators have shifted to adding ionic liquid (IL) to block copolymers or Nafion as a way to replace the water with a more electrochemically stable and nonvolatile fluid.[35–37] Electronically conductive polymers[38] have also been investigated, notably polypyrrole[39–45] and poly(3,4-ethylenedioxythiophene)-poly(styrenesulfonate) (PEDOT:PSS),[46,47] which generally exhibit bending strains <1%.[39,40]

Despite years of study, the key material parameters which govern ionic polymer actuation are still unclear. In dielectric elastomers, it is known that actuation pressures scale proportionally with the dielectric constant and inversely with Young's modulus (E).[17] However, for ionic polymers, the fields are orders of magnitude lower and electrostriction is not expected to play a major role. Higher ionic conductivity appears to generate a faster response, while the roles of other factors such as glass transition temperature (T_g), modulus, and polarity have not been systematically investigated. Most studies on ionic soft actuators focus on one particular polymer (Nafion,[31–33,48,49] poly(vinylidene fluoride) (PVDF),[8,41,50,51] Nexar,[52] or custom block copolymers[35,36]) with a small molecule additive such as water, IL, or organic solvent. Although Nafion has been studied with a range of ILs[37,53] solvents,[49] and salt solutions,[54] the comparisons

C. Shen, Q. Zhao, Prof. C. M. Evans
Frederick Seitz Materials Research Laboratory (MRL)
University of Illinois at Urbana-Champaign (UIUC)
IL 61801, USA
E-mail: cme365@illinois.edu
C. Shen
Department of Chemistry
University of Illinois at Urbana-Champaign (UIUC)
IL 61801, USA
Q. Zhao, Prof. C. M. Evans
Department of Materials Science and Engineering
University of Illinois at Urbana-Champaign (UIUC)
IL 61801, USA
Prof. C. M. Evans
Beckman Institute for Advanced Science and Technology
University of Illinois at Urbana-Champaign (UIUC)
IL 61801, USA
The ORCID identification number(s) for the author(s) of this article can be found under https://doi.org/10.1002/admt.201800535.

DOI: 10.1002/admt.201800535

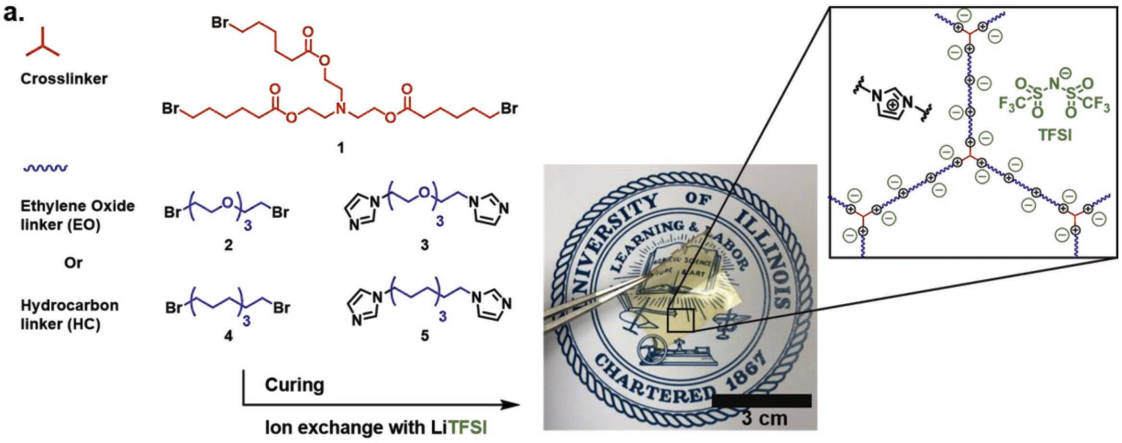

b.

Network	T_g (°C)	T_d (°C)	Water uptake (wt.%)	Ionic conductivity (10^{-6} S/cm)	Young's modulus (MPa)
25 % HC TFSI	- 33	377	0.2%	7.28 ± 0.6	0.792 ± 0.098
25 % EO/HC TFSI	- 40	380	0.2%	16.7 ± 2.5	0.274 ± 0.039
25 % EO TFSI	- 40	400	0.6%	31.0 ± 4.5	0.118 ± 0.019
33 % EO TFSI	- 40	375	0.4%	24.4 ± 3.1	0.277 ± 0.005
50 % EO TFSI	- 40	362	0.5%	19.4 ± 4.2	0.692 ± 0.040
100 % EO TFSI	- 36	365	0.5%	11.0 ± 2.2	1.829 ± 0.075

Figure 1. a) Monomers used to synthesize n-PILs with either HC or EO linkers. The reaction is run overnight at 80 °C to cure the networks followed by ion exchange to the imidazolium TFSI form which is flexible and transparent as shown in the inset photo. b) Thermal transitions, water uptake, ionic conductivity, and modulus for the n-PILs investigated in this work. The percentages indicate the number of ionic sites formed from tribromo species relative to dibromo monomers. The monomers are either all HC or EO except for 25% EO/HC which is a 43/57 mixture.

between groups employed different voltages, frequencies, and sample dimensions which are critical for making direct comparisons. Larger tip displacements will be observed in thinner samples (50 µm)[32] while higher forces/smaller displacements are observed in thicker samples (≈2 mm)[49] of the same material.

Here, we present the development of a new class of actuating polymer comprised of crosslinked network polymerized ionic liquids (n-PILs) with tethered imidazolium cations and mobile bis(trifluoromethane sulfonimide) (TFSI) anions. The n-PIL actuators exhibit performance comparable to hydrated or IL doped systems but without the need for small molecule additives. These networks are made via a facile step growth route and have highly tunable polarity and modulus through the choice of either hydrocarbon (HC) or ethylene oxide (EO) monomers and crosslinking density. The T_g is not substantially affected by monomer choice, and the role of conductivity, crosslinking, and modulus can be probed to understand how they systematically affect actuation. Because the n-PILs are hydrophobic (<1 wt% water uptake under ambient conditions), they can be operated over thousands of cycles at 3 V with minimal degradation of performance. Additionally, the leaching of ionic liquids or other small molecule additives is suppressed which may make them suitable for wearable applications, although human testing has not yet been performed. To our knowledge, only one very recent study has reported actuation for a dry, linear PIL.[55] However, this work did not investigate structure–performance relationships, exhibited a ten times slower actuation, and had lower strain than in the present work.

A series of n-PILs with different linker polarities, either HC or EO, and a range of crosslinking densities were synthesized to probe how molecular details impact actuation. As shown in **Figure 1**, all networks contain the same tribromo crosslinker (**1**), dibromo monomers (**2**, **4**), and a stoichiometric ratio of diimidazole monomers (**3**, **5**) containing either HC (11 atoms) or EO (also 11 atoms) between the end groups. The monomer syntheses are based on well-known reactions and are reported in the Supporting Information with characterization (Figure S1). By varying ratios of crosslinker to difunctional monomers, networks were prepared with four different crosslinking densities of 25, 33, 50, and 100 mol%. A crosslinking percent of 25% corresponds to a sample where 25% of the imidazolium cations were formed by reaction with a crosslinker and 75% with a dibromo species. The percent is set by the stoichiometry of the reaction mixture and solid-state NMR indicates a high conversion network (Figure S2, Supporting Information). Three different linker chemistry ratios (0, 43, and 100 mol% EO with the balance being HC) were also synthesized with a fixed crosslinking density of 25% to investigate linker polarity effects. All samples were ion exchanged to TFSI counterions which are known to plasticize imidazolium ionic liquids resulting in higher ionic conductivity, larger electrochemical stability window, and lower T_g (≈–40 °C).[53,56] The TFSI exchange was monitored by elemental analysis (Tables S1 and S2, Supporting Information) and Br content (from both unreacted bromo end groups and Br anions) is <0.6 wt% in all networks, putting a lower bound on the network conversion and ion exchange efficiency. Current theories[57,58] for actuation in single ion conductors indicate that the size of the mobile ion limits the concentration of charges which can accumulate at an electrode and creates a volumetric mismatch between the double layer and depletion layers which form at opposing electrodes. Thus, large anions such as

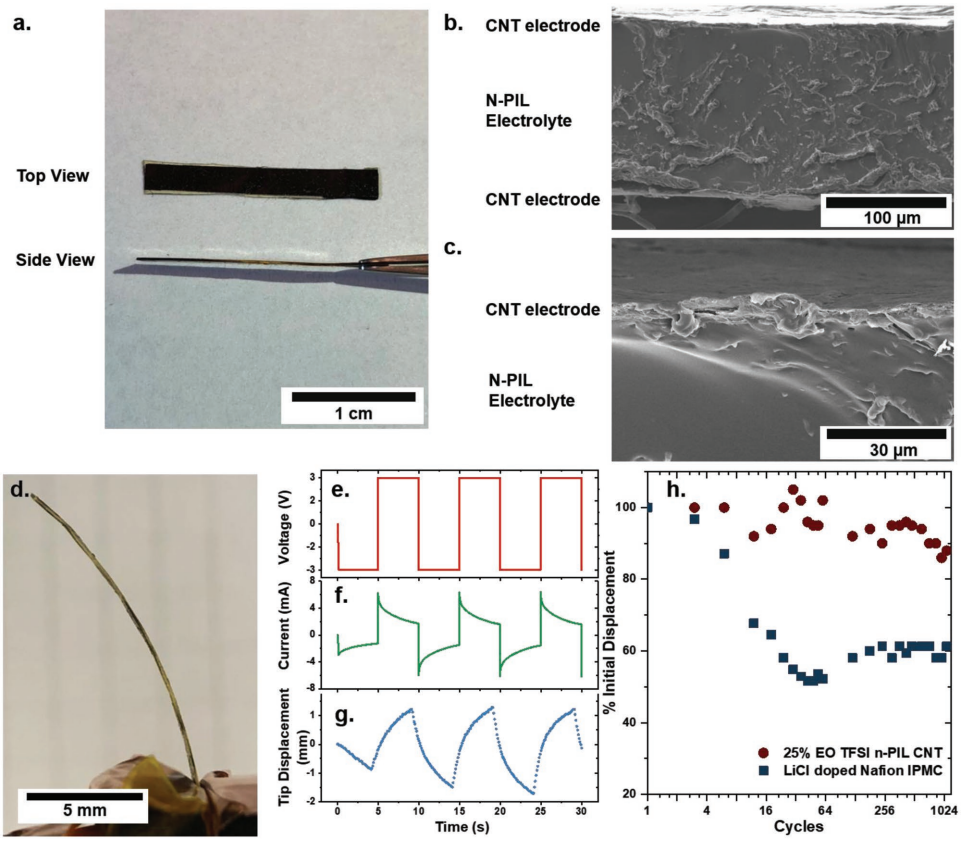

Figure 2. a) Top and side view photos of n-PIL actuators fabricated with CNT electrodes with no voltage stimulus. b) Scanning electron microscope image of the cross-section of a 25% EO n-PIL actuator with CNT electrodes on top and bottom surfaces. c) A zoomed in view of the top polymer–electrode interface of the composite device in panel (b). d) A photograph of 25% EO TFSI actuator reaches maximum displacement under 3 V potential after 2 mins. e) Actuation of a 25% EO n-PIL actuator in response to a 3 V, 0.1 Hz square wave. The corresponding f) current and g) tip displacement are also plotted. h) The displacements of n-PIL and saturated LiCl solution doped Nafion IPMC actuators cycling under 3 V, 0.1 Hz testing conditions. The *y*-axis represents the % displacement with respect to the first cycle.

TFSI (calculated volume of 147 $Å^3$)[59] are anticipated to generate greater actuation response than smaller anions such as Br (5.9 $Å^3$).

Due to their high-surface area, low resistivity, and good flexibility, thin (20 µm) single walled carbon nanotube (CNT) sheets are fabricated and used as the compliant electrodes of n-PILs in this study. **Figure 2**a shows top and side view photos of an assembled actuator after sandwiching a layer of n-PIL in between two CNT electrodes under pressure. The black surface is the color of the CNT sheet. Scanning electron microscope images of the cross-section of an n-PIL actuator (Figure 2b) show the three-layer structure. A zoomed in image of the top n-PIL-CNT interface (Figure 2c) indicates that only ≈5 µm of the CNT sheet is exposed. The rest of the CNT (≈15 µm) is completely immersed into the polymer matrix creating a large polymer–electrode interface for ion accumulation. Electroless plating of metal particles from metal salts, a method widely used in Nafion IPMCs, was also tested on n-PILs. Since the networks contain base sensitive ester linkages, n-PILs did not survive the reduction process even with reducing agents such as ammonium hydroxide or hydrazine. A number of other electrodes (e.g., metal nanoparticles, sputtered gold) were also tested during the development of the n-PIL actuators, and CNT electrodes showed the best performance.

The electrochemical stability of all networks in this study is sufficient to allow repeated testing at 3 V (verified by cyclic voltammetry (CV) scans, Figure S3, Supporting Information) as expected for imidazolium TFSI systems. Redox reactions are observed when the potential exceeds >± 3 V limiting the window for sustained actuation. The n-PIL actuators were tested at ambient conditions (22 °C, ≈50% relative humidity (RH)) by lightly clamping between two copper foil electrodes which allow the attachment of clamps (Figure S9, Supporting Information). A potentiostat was then used to apply a 3 V, 0.1 Hz square wave alternating current (AC) potential (Figure 2e). As the actuator bent, the tip displacement was recorded with a laser sensor. The current and tip displacement of the best performing n-PIL comprised entirely of EO difunctional monomers **2** and **3** with a 25% crosslinking density are shown in Figure 2f,g. This sample exhibited a tip-to-tip displacement of 3.1 ± 0.6 mm (with error bars being determined from three independently prepared actuators) at 0.1 Hz which is comparable to the hydrated or IL swollen Nafion with similar thickness and area (to be discussed later). The current reflects electrode polarization (EP) and is analogous to the charging behavior of a double layer capacitor. The displacement evolves steadily as EP occurs and mobile TFSI anions accumulate at the positive electrode and

deplete from the negative electrode leading to a volume mismatch which causes bending. Additionally, the presence of a layer of negative TFSI anions leads to charge repulsion at the positive electrode which further contributes to the bending. The AC measurements limit the time over which EP can occur and are influenced by ionic conductivity. The n-PIL actuators were also tested under a 3 V direct current (DC) potential where the tip was allowed to deflect until it reached a steady value with a maximum displacement of 6.7 ± 0.6 mm (Figure 2d) to reach an equilibrium displacement. No back relaxation was observed, a distinct advantage over Nafion, and other hydrated polymer actuators. All displacement data are reported from an average of at least three individually prepared samples which showed excellent reproducibility (Table S3, Supporting Information).

A major advantage of the n-PIL actuators is that they have no solvent and low water uptakes. Thus, water splitting and solvent breakdown are not issues when cycling. Figure 2h shows the displacement of our 25% crosslinked EO actuator which started at 3.1 mm and decayed to ≈95% over ≈500 cycles. After 1000 cycles, the displacement eventually dropped to ≈85% of the original value. As a comparison, a Nafion IPMC actuator was fabricated following a literature reported procedure with electroless plating of Pt electrodes.[46] The Nafion IPMC was doped with a saturated LiCl solution and the initial tip-to-tip displacement was 3.4 mm (at 3 V, 0.1 Hz) in agreement with prior literature. Upon cycling, the displacement quickly deteriorated to around 50% of original performance in less than 50 cycles which we attribute to water splitting and/or dehydration effects. This lowers the conductivity and flexibility of the system and compromises the performance of the Nafion IPMC actuator. Typically, Nafion cycling experiments are performed at 1 V.[35] After 1000 cycles, a 3 V DC potential was applied to both systems with the Nafion showing 5.0 mm of displacement, and a 25% crosslinked EO network exhibiting 6.0 mm of displacement. Thus, the n-PILs outperformed Nafion after cycling under the same conditions.

As mentioned in the introduction, the roles of polarity, modulus, conductivity, and T_g on actuation are not well understood in ionic polymer actuators. To explore the structure-performance relationship of n-PILs, the crosslinking density and linker chemistry were systematically varied to identify their relative importance. The thermal, mechanical, and conductive properties of all n-PIL samples are reported in Figure 1b. Thermal properties are largely unaffected across networks with varying EO/HC content or crosslinking density. As shown in Figure 1b and S4 in the Supporting Information, all n-PILs have thermal stability >360 °C. Furthermore, all the networks have a T_g of –40 °C except for the 25% HC system (–33 °C), and the 100% EO system (–36 °C) indicating that T_g is not changing appreciably (Figure 1b and S5, Supporting Information). Thus, T_g is not playing a primary role in subsequent actuation trends. Water uptakes are all below 1 wt% regardless of linker chemistry (Figure 1b and S6, Supporting Information) due to the hydrophobic nature of the TFSI anion which leads to greater cyclability relative to Nafion systems (Figure 2h) and should also allow for higher temperature actuation without dehydration or degradation (which occurs above 360 °C).

Conductivity, measured under ambient conditions, monotonically increases by a factor of three in the EO systems as the crosslinking density decreases from 100% to 25% (Figure 3b and S7, Supporting Information). Thus, even though T_g and water uptake are not changing substantially, the crosslinking density appears to influence the conductivity. The ionic conductivity increases by a factor of five in the 25% crosslinked networks, as the monomers are varied from all HC to all EO, due to the increased polarity of the medium. Further work is needed to understand the role of mesh size and network polarity on ion aggregation and conductivity.

One of the key properties which was investigated for the networks is the E. For dielectric elastomer actuators,[17] the strain decreases as $1/E$ but such systems work based on a different mechanism, electrostriction. For the n-PILs, lower crosslinking density corresponds to lower modulus and all networks have $E < 1$ MPa except for the 100% crosslinking density sample (Figure 1b). **Figure 3**g shows the stress–strain curves which are linear and have an increasing slope (modulus) with increasing crosslinking density for the EO networks. In fact, these materials can be stretched to >100% in the case of low crosslinking density (Figure S8, Supporting Information) and such flexible, rubbery polymers are anticipated to be beneficial for application as wearable actuators. Upon changing the network chemistry from HC to EO, the modulus decreases by a factor of 7.

Figure 3a–c examine the role of crosslinking density on modulus, ionic conductivity, and actuator displacement under both DC and AC potentials. As mentioned, T_g does not change appreciably in these networks and thus is not included in subsequent discussion. The 25% crosslinking density EO network has the largest average tip displacement of 6.7 ± 0.6 mm under 3 V DC potential and an average of 3.1 ± 0.6 mm tip-to-tip displacement under a 0.1 Hz, 3 V AC potential. Upon increasing the crosslinking density to 33, 50, and ultimately 100% the displacement systematically decreases to <1 mm at full crosslinking for both AC and DC testing conditions. The ionic conductivity also systematically decreases with increasing crosslinking density. Conductivity is important for the AC response as it determines the rate of ion transport from one electrode to the other and the charging/ion accumulation kinetics. There is a clear correlation of conductivity and tip displacement outside of experimental error which was anticipated. The DC actuation response cannot be explained in terms of conductivity because, after a sufficient time, ion accumulation will saturate. Instead, the difference in DC displacement is attributed to variations in modulus. A softer material is easier to deform with a given pressure generated by the ion accumulation process. With increasing E, displacement decreases which is qualitatively consistent with nonionic polymer dielectric actuators. A plot of displacement versus $1/E$ reveals an apparent nonlinear relationship for AC tests, presumably due to the role of ion conduction and accumulation which has not equilibrated on the 0.1 Hz timescale (Figure 3i). This is an important insight for ionic polymer actuators which are frequently tested and used in an AC mode. In contrast, the displacement is linear in $1/E$ for DC measurements, where ionic conductivity no longer plays a role, which is anticipated for equilibrium bending. This suggests future routes to engineer the displacement through tuning the mechanical properties via crosslinking, higher functionality crosslinkers, and softer/harder linkers. Overall, Figure 3 indicates that both higher ionic conductivity and lower modulus are contributing to the tenfold performance difference between the 25% EO and 100% EO n-PIL actuators under AC conditions.

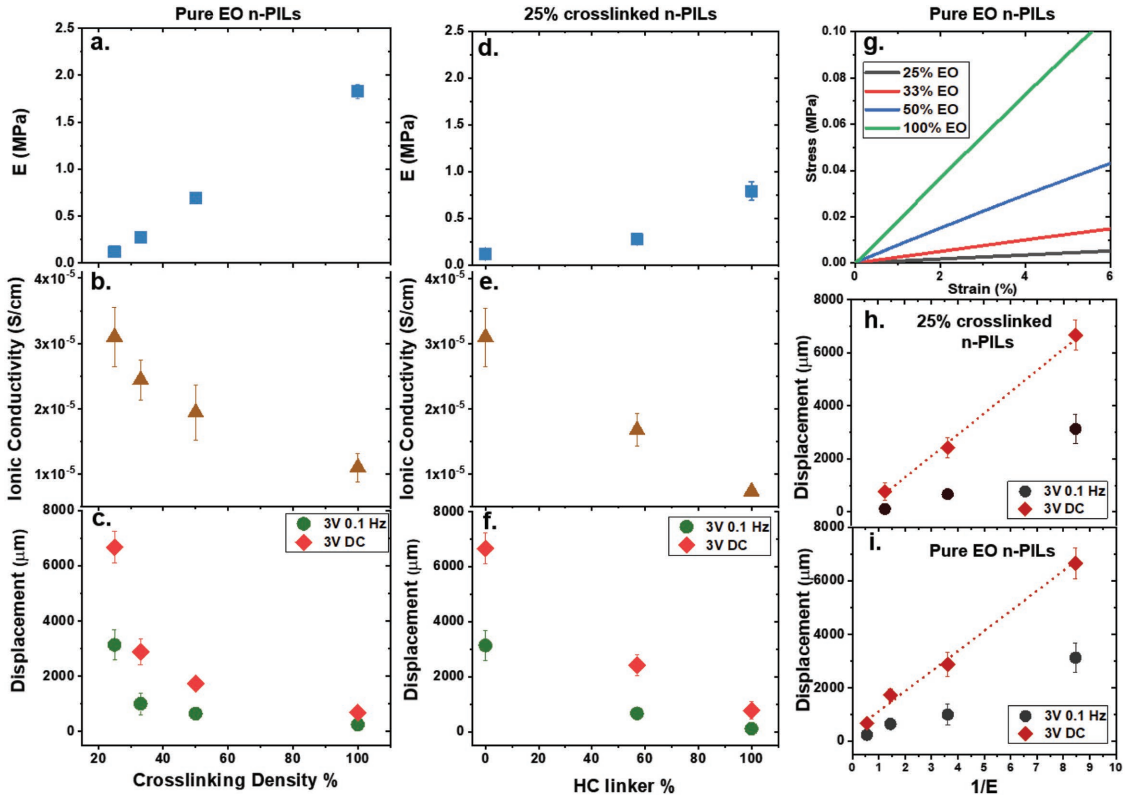

Figure 3. Dependence of a) *E* and b) ionic conductivity on c) displacement of all EO actuators as a function of crosslinking density. Dependence of d) *E*, e) ionic conductivity, f) displacement of actuators with 25% crosslinked mixed EO/HC linkers. The DC displacements are relative to the straight beam, while AC measurements are reported as tip-to tip displacements. g) Stress–strain curves of pure EO n-PILs with different crosslinking density. h) Relationship between 1/*E* and tip displacement with 25% crosslinked full HC, mixed EO/HC, and full EO networks (left to right). i) Relationship between 1/*E* and tip displacement with 100%, 50%, 33%, and 25% all EO networks (left to right). Dotted lines are fitting function that demonstrate linearity. Experimental data with errors are listed in Table S3 in the Supporting Information. Error bars in the above graphs indicating error coming from three or more individually prepared samples/actuators.

The other molecular variable investigated was the effect of linker polarity on actuator performance. It is well known that polar EO provides better solvation for ions than nonpolar HC.[60] For a systematic comparison, the HC and EO linkers both contained 11 atoms and thus had the same ionic concentration and only varied in polarity. At 25% crosslinking density, the EO network has a lower T_g, lower modulus and higher ionic conductivity than the corresponding HC linker network. A 43/57 mixture of EO/HC had intermediate properties to the two pure networks. In the case of the EO network, the combined effect of both low modulus and high conductivity allows the EO actuator to demonstrate a 30-fold increase of displacement as compared to the HC actuator (Figure 3d–f). Higher conductivity, related to faster segmental dynamics and higher polarity, contributes to the improved AC displacement, while low modulus allows for greater actuator tip displacement at a constant potential (Figure 3f,h).

It is interesting to note that the highest ionic conductivity observed was 3×10^{-5} S cm^{-1} at ambient conditions (25% EO network) which is much lower than that of Nafion (≈0.1 S cm^{-1}). However, for 0.1 Hz actuation this does not appear to cause substantial differences in displacement. Nafion is known to show a maximum at a higher resonant frequency (≈30 Hz) which may be related to the higher conductivity and future work should investigate high frequency actuation in the n-PILs. Nafion also has a higher modulus which may be impeding actuation, as observed in our networks, despite the higher conductivity.[26] Decoupling the roles of modulus and conductivity is difficult in such systems due to the lack of tunability of the polymer structure. In contrast, our networks can serve as model platforms to uncover fundamental structure-performance relationship in ionic polymer actuators.

In the literature, ionic polymer actuators are made in various dimensions which can make comparisons less straightforward. To place our n-PILs in the context of prior work, the strain (ε) is calculated using the relation $\varepsilon = (2dt)/(L^2 + d^2)$, where d is the tip displacement, t is the thickness, and L is the distance away from the clamp where the displacement measurement takes place. For the 25% EO actuator (0.17 mm thick, displacement measured 15 mm from the clamp), a tip displacement of 6.7 ± 0.6 mm at 3 V DC corresponds to $\varepsilon = 0.9\%$. Next, we identified the best performing ionic polymer actuators from the literature and calculated their strains using dimensions provided in the references. We have intentionally omitted reports with testing conditions above 5 V or that are above the electrochemical window of the electrolyte materials (aqueous solutions, ILs, Nafion, conducting polymers, etc.) and thus will not be cyclable. As seen in **Figure 4**, the best strain observed in

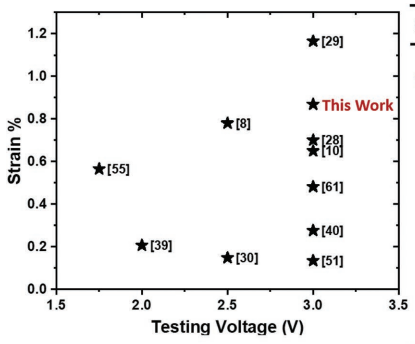

Reference	Strain %	Electrolyte	Displacement (d), thickness (t), free length (L) (mm)
[29]	1.13	Sulfonated PS blockcopolymer, IL	6.3, 0.07, 6
This Work	0.87	n-PIL, DRY	7, 0.17, 15
[8]*	0.78	PVDF, IL	16, 0.08, 11
[28]	0.70	Sulfonated PS block copolymer, Zwitterion	14.5, 0.08, 11
[10]	0.65	Sulfonated PS block copolymer, IL	Not specified, strain reported by author
[55]	0.56	Linear PIL, DRY	0.15, 0.17, 3
[61]	0.40	PAA network, IL	10, 0.1, 20
[40]	0.28	Sulfonated polyimide, IL	10, 0.1, 25
[39]	0.21	Cellulose, IL	6.5, 0.15, 30
[51]	0.13	Sulfonated PEEK, PVDF, IL	2.5, 0.24, 30
[30]	0.08	Nafion, IL	2, 0.23, 35

Figure 4. Bending strains calculated for this work and literature references based on reported sample dimensions at an operation voltage of 3 V or lower. *Actuator from ref. [8] was tested under 0.1 Hz, while all other displacement data are obtained at maximum displacement under steady potential. Samples with aqueous solutions or operating above the electrolyte stability window have been intentionally omitted due to cyclability issues.

our n-PILs actuators (0.9% at 3 V, DC) is only outperformed by a block copolymer doped with free ionic liquid which exhibit 1.1% (also at 3 V DC).[36] As mentioned, free IL may leach out over time in particular if worn on the skin or under stress. Nevertheless, the copolymer work is impressive and suggests that nanophase separation may be a useful strategy for further optimization of our n-PIL electrolyte. The only other undoped system reported in the literature is a linear PIL which generates less than 0.6% strain in 20 mins (at 1.75 V, the highest reported voltage),[55] whereas the present n-PIL is able to reach 0.9% strain in 2 mins (at 3 V). In our experience, linear PILs with high conductivity are also low viscosity which motivates the use of network PILs. It is worth noting that Figure 4 does not provide frequency information which is important for some applications.

In conclusion, a new class of electroactive polymer was designed and synthesized based on n-PILs which exhibit low T_g (≈ −40 °C), moderate ionic conductivity (≈10^{-5} S cm^{-1} under ambient conditions), low stiffness (E < 1 MPa), large electrochemical window (±3 V), and high thermal stability (T_d > 360 °C) for the development of soft, low voltage, dopant-free polymer actuators. The n-PIL actuators showed large deformation under both AC and DC testing conditions without the need of salt solutions or free ILs. As a result, these actuators showed only a 15% drop in tip displacement after 1000 cycles at 3 V, 0.1 Hz, in contrast to Nafion IPMCs which show a 45% performance deterioration after 50 cycles under the same testing condition. Because the n-PILs are custom synthesized using monomers of precise length and polarity, the networks were engineered to probe structure-actuation relationships. An order of magnitude displacement increase was observed by lowering the crosslinking density from 100% to 25% and switching from HC to EO monomers. Both modulus and ionic conductivity are hypothesized to be responsible for these substantial changes in tip displacement under an AC potential, while modulus alone appears to dictate the DC response. It is found that displacement does not scale linearly with $1/E$ for AC measurements, while DC measurements do exhibit a linear relationship. This is a key insight for designing and using ionic polymer actuators. The dry 25% EO actuator shows a bending strain of ≈0.9% which is comparable to the best performing ionic polymer actuators, and is only slightly less than 1.1% for IL doped block copolymer actuators under similar testing conditions.[36] Such dopant-free, polymer actuators are ideal candidates for next-generation artificial muscles, soft robotics, and wearable devices. Future work is underway probing heterogeneous networks, a broader range of starting monomers, and variations of electrodes to further optimize the performance.

Experimental Section

The detailed procedures for monomer synthesis, network curing, actuator testing, thermogravimetric analysis (TGA), differential scanning calorimetry (DSC), impedance, CV scans and elemental analysis are provided in Figures S1–S9 and Tables S1–S3 in the Supporting Information.

Supporting Information

Supporting Information is available from the Wiley Online Library or from the author.

Acknowledgements

This work was supported by funding from Facebook and the Materials Science and Engineering Department at the University of Illinois, Urbana-Champaign. This work was carried out in part in the Materials Research Laboratory Central Research Facilities, University of Illinois. The authors acknowledge Prof. Paul V. Braun for helpful discussions.

Conflict of Interest

The authors declare no conflict of interest.

Keywords

actuator, molecular design, polymerized ionic liquid, structure–performance relationship

Received: October 16, 2018
Revised: November 2, 2018
Published online: December 4, 2018

[1] R. L. Truby, M. Wehner, A. K. Grosskopf, D. M. Vogt, S. G. M. Uzel, R. J. Wood, J. A. Lewis, *Adv. Mater.* **2018**, *30*, 1706383.
[2] R. Tabassian, J. Kim, V. H. Nguyen, M. Kotal, I. K. Oh, *Adv. Funct. Mater.* **2018**, *28*, 1705714.
[3] J. K. Sun, W. Y. Zhang, R. Guterman, H. J. Lin, J. Y. Yuan, *Nat. Commun.* **2018**, *9*, 1717.
[4] M. Schaffner, J. A. Faber, L. Pianegonda, P. A. Ruhs, F. Coulter, A. R. Studart, *Nat. Commun.* **2018**, *9*, 878.
[5] S. Poppinga, C. Zollfrank, O. Prucker, J. Ruhe, A. Menges, T. Cheng, T. Speck, *Adv. Mater.* **2018**, *30*, 1703653.
[6] D. M. Opris, *Adv. Mater.* **2018**, *30*, 1703678.
[7] C. X. Ma, W. Lu, X. X. Yang, J. He, X. X. Le, L. Wang, J. W. Zhang, M. J. Serpe, Y. J. Huang, T. Chen, *Adv. Funct. Mater.* **2018**, *28*, 1704568.
[8] C. Lu, Y. Yang, J. Wang, R. P. Fu, X. X. Zhao, L. Zhao, Y. Ming, Y. Hu, H. Z. Lin, X. M. Tao, Y. L. Li, W. Chen, *Nat. Commun.* **2018**, *9*, 752.
[9] A. Kotikian, R. L. Truby, J. W. Boley, T. J. White, J. A. Lewis, *Adv. Mater.* **2018**, *30*, 1706164.
[10] S. J. Kim, O. Kim, M. J. Park, *Adv. Mater.* **2018**, *30*, 17106547.
[11] T. Guin, M. J. Settle, B. A. Kowalski, A. D. Auguste, R. V. Beblo, G. W. Reich, T. J. White, *Nat. Commun.* **2018**, *9*, 2531.
[12] T. N. Do, H. Phan, T. Q. Nguyen, Y. Visell, *Adv. Funct. Mater.* **2018**, *28*, 1800244.
[13] S. M. Chin, C. V. Synatschke, S. P. Liu, R. J. Nap, N. A. Sather, Q. F. Wang, Z. Alvarez, A. N. Edelbrock, T. Fyrner, L. C. Palmer, I. Szleifer, M. O. de la Cruz, S. I. Stupp, *Nat. Commun.* **2018**, *9*, 2395.
[14] T. T. Chen, H. Bakhshi, L. Liu, J. Ji, S. Agarwal, *Adv. Funct. Mater.* **2018**, *28*, 1800514.
[15] L. Belding, B. Baytekin, H. T. Baytekin, P. Rothemund, M. S. Verma, A. Nemiroski, D. Sameoto, B. A. Grzybowski, G. M. Whitesides, *Adv. Mater.* **2018**, *30*, 1704446.
[16] E. Acome, S. K. Mitchell, T. G. Morrissey, M. B. Emmett, C. Benjamin, M. King, M. Radakovitz, C. Keplinger, *Science* **2018**, *359*, 61.
[17] R. Pelrine, R. Kornbluh, Q. B. Pei, J. Joseph, *Science* **2000**, *287*, 836.
[18] R. Pelrine, R. Kornbluh, G. Kofod, *Adv. Mater.* **2000**, *12*, 1223.
[19] M. Duduta, R. J. Wood, D. R. Clarke, *Adv. Mater.* **2016**, *28*, 8058.
[20] S. Shian, R. M. Diebold, D. R. Clarke, *Opt. Express* **2013**, *21*, 8669.
[21] H. Okuzaki, T. Kuwabara, K. Funasaka, T. Saido, *Adv. Funct. Mater.* **2013**, *23*, 4400.
[22] Y. Q. Gu, N. S. Zacharia, *Adv. Funct. Mater.* **2015**, *25*, 3785.
[23] Q. Zhao, J. Heyda, J. Dzubiella, K. Tauber, J. W. C. Dunlop, J. Y. Yuan, *Adv. Mater.* **2015**, *27*, 2913.
[24] Q. Zhao, J. W. C. Dunlop, X. L. Qiu, F. H. Huang, Z. B. Zhang, J. Heyda, J. Dzubiella, M. Antonietti, J. Y. Yuan, *Nat. Commun.* **2014**, *5*, 4293.
[25] L. D. Zhang, P. Naumov, X. M. Du, Z. G. Hu, J. Wang, *Adv. Mater.* **2017**, *29*, 1702231.
[26] M. Behl, K. Kratz, U. Noechel, T. Sauter, A. Lendlein, *Proc. Natl. Acad. Sci. USA* **2013**, *110*, 12555.
[27] L. D. Zarzar, P. Kim, J. Aizenberg, *Adv. Mater.* **2011**, *23*, 1442.
[28] M. Shahinpoor, Y. Bar-Cohen, J. O. Simpson, J. Smith, *Smart Mater. Struct.* **1998**, *7*, R15.
[29] M. Shahinpoor, K. J. Kim, *Smart Mater. Struct.* **2001**, *10*, 819.
[30] A. J. Duncan, D. J. Leo, T. E. Long, *Macromolecules* **2008**, *41*, 7765.
[31] H. L. He, J. P. Wang, *Adv. Mater. Processes* **2011**, *311–313*, 2000.
[32] S. Liu, Y. Liu, H. Cebeci, R. G. de Villoria, J. H. Lin, B. L. Wardle, Q. M. Zhang, *Adv. Funct. Mater.* **2010**, *20*, 3266.
[33] Z. C. Zhu, H. L. Chen, B. Li, Y. Q. Wang, *Manuf. Sci. Eng.* **2010**, *97–101*, 1590.
[34] D. Pugal, S. J. Kim, K. J. Kim, K. K. Leang, *Electroact. Polym. Actuators Devices* **2010**, *7642*, 76420U.
[35] O. Kim, H. Kim, U. H. Choi, M. J. Park, *Nat. Commun.* **2016**, *7*, 13576.
[36] O. Kim, T. J. Shin, M. J. Park, *Nat. Commun.* **2013**, *4*, 2208.
[37] I. W. P. Chen, M. C. Yang, C. H. Yang, D. X. Zhong, M. C. Hsu, Y. W. Chen, *ACS Appl. Mater. Interfaces* **2017**, *9*, 5550.
[38] E. Smela, *Adv. Mater.* **2003**, *15*, 481.
[39] A. Khaldi, A. Maziz, G. Alici, G. M. Spinks, E. W. H. Jager, *Electroact. Polym. Actuators Devices* **2015**, *9430*, 94301R.
[40] A. Maziz, C. Plesse, C. Soyer, C. Chevrot, D. Teyssie, E. Cattan, F. Vidal, *Adv. Funct. Mater.* **2014**, *24*, 4851.
[41] B. Gaihre, G. Alici, G. M. Spinks, J. M. Cairney, *J. Microelectromech. Syst.* **2012**, *21*, 574.
[42] L. Bay, K. West, P. Sommer-Larsen, S. Skaarup, M. Benslimane, *Adv. Mater.* **2003**, *15*, 310.
[43] G. M. Spinks, L. Liu, G. G. Wallace, D. Z. Zhou, *Adv. Funct. Mater.* **2002**, *12*, 437.
[44] C. F. Smith, S. C. Yang, T. E. Long, S. Priya, *Electroact. Polym. Actuators Devices* **2011**, *7976*, 797625.
[45] Y. Tadesse, J. Brennan, C. Smith, T. E. Long, S. Priya, *Electroact. Polym. Actuators Devices* **2010**, *7642*, 764222.
[46] S. S. Kim, J. H. Jeon, H. I. Kim, C. D. Kee, I. K. Oh, *Adv. Funct. Mater.* **2015**, *25*, 3560.
[47] R. K. Cheedarala, J. H. Jeon, C. D. Kee, I. K. Oh, *Adv. Funct. Mater.* **2014**, *24*, 6005.
[48] S. Liu, W. J. Liu, Y. Liu, J. H. Lin, X. Zhou, M. J. Janik, R. H. Colby, Q. M. Zhang, *Polym. Int.* **2010**, *59*, 321.
[49] H. S. Wang, J. Cho, D. S. Song, J. H. Jang, J. Y. Jho, J. H. Park, *ACS Appl. Mater. Interfaces* **2017**, *9*, 21998.
[50] J. Lu, S. G. Kim, S. Lee, I. K. Oh, *Adv. Funct. Mater.* **2008**, *18*, 1290.
[51] J. H. Jeon, S. P. Kang, S. Lee, I. K. Oh, *Sens. Actuators, B* **2009**, *143*, 357.
[52] R. L. Gao, D. Wang, J. R. Heflin, T. E. Long, *J. Mater. Chem.* **2012**, *22*, 13473.
[53] M. D. Bennett, D. J. Leo, *Sens. Actuators, A* **2004**, *115*, 79.
[54] B. J. Landi, R. P. Raffaelle, M. J. Heben, J. L. Alleman, W. VanDerveer, T. Gennett, *Nano Lett.* **2002**, *2*, 1329.
[55] F. B. Ribeiro, C. Plesse, G. T. M. Nguyen, S. M. Morozova, E. Drockenmuller, A. S. Shaplov, F. Vidal, *Proc. SPIE* **2018**, *10594*, 10594.
[56] H. Ohno, *Electrochim. Acta* **2001**, *46*, 1407.
[57] A. A. Lee, R. H. Colby, A. A. Kornyshev, *Soft Matter* **2013**, *9*, 3767.
[58] A. A. Lee, R. H. Colby, A. A. Kornyshev, *J. Phys.: Condens. Matter* **2013**, *25*, 082203.
[59] M. A. Ratner, D. F. Shriver, *Chem. Rev.* **1988**, *88*, 109.
[60] M. M. A. Ue, S. Nakamura, *J. Electrochem. Soc.* **2002**, *149*, A1385.
[61] Y. Yan, T. Santaniello, L. G. Bettini, C. Minnai, A. Bellacicca, R. Porotti, I. Denti, G. Faraone, M. Merlini, C. Lenardi, P. Milani, *Adv. Mater.* **2017**, *29*, 1606109.